

Effect of compressive strain on electric resistance of multi-wall carbon nanotube networks

Running header: Effect of compressive strain on electric resistance of multi-wall carbon nanotube networks

ABSTRACT

The network of entangled multiwall carbon nanotubes is shown to be a conductor whose resistance is sensitive to compressive strain both in the course of strain growth and when loading/unloading cycles are imposed. The cycles at first lead to the resistance decrease but with a higher number of cycles they fade away. To model the resistance/strain dependence, it is hypothesized that compression increases local contact forces between nanotubes and bends the nanotubes, which results in more conducting contacts. The lack of detailed knowledge of these mechanisms as well as an unclear shift from individual contacts description to the whole network resistance is circumvented using the statistical approach. In this respect, good data representation is reached using Weibull and Levy-stable distribution for the description of distribution of nanotubes contact resistances and contact formation, respectively.

1 Introduction

Recent technology progress relies heavily on the use of materials that can offer advanced structural and functional capabilities. In this respect, entangled carbon nanotube (CNT) network structures of buckypaper show a great potential for developing high-performance polymer composite materials. The networks can proportionally transfer their unique properties into composites and bring substantial improvements in structural strength, electrical and thermal conductivity, electromagnetic interference shielding and other properties in comparison to polymer composites with carbon nanotubes particulate filling [1,2].

The first CNT network was fabricated when nanotubes were dispersed into a liquid suspension and then filtered through a fine filtrating mesh [3]. Consequently, the pure nanotubes stuck to one another and formed a thin intertwined freestanding structure, later dubbed buckypaper. The aim of this study is to explore the electrical resistance of multi-wall carbon nanotubes (MWNT) network structure of buckypaper under compression. The inspiration among others offers the recent paper on the electric resistance of freely poured CNT tangles under compression in which the resistance/compression dependence and the contact resistance between nanotubes is thoroughly evaluated [4]. However, the thickness of investigated powdery CNT layers in a tubular glass cell is about 2.5 mm. On the other hand, the CNT network structure of buckypaper is purposely thin (~100 μm) since it is primarily intended as CNT matting for polymer composite fabrication. Thus the sense of resistance/compressive strain testing of the MWNT network structure is to reveal the sensitivity of resistance to compression of the network in itself but at the same time as an important structural element of conductive MWNT/polymer composite.

Experimental

Purified MWNT of acetylene type were supplied by Sun Nanotech Co. Ltd., China. According to the supplier the nanotube diameter is 10-30 nm, length 1-10 μm , purity >90% and volume resistance 0.12 Ωcm .  ??????

The nanotubes as received were used for the preparation of aqueous paste: 1.6 g of MWNT and ~ 50 ml of deionized water were mixed with the help of a mortar and pestle. The paste was diluted in deionized water with sodium dodecyl sulfate (SDS) and 1-pentanol. Then NaOH solved in water was added to adjust pH to the value of 10 [5]. The final nanotube concentration in the dispersion was 0.3 wt.%, concentration of SDS and 1-pentanol 0.1M and 0.14M, respectively [6]. The dispersion was sonicated in Dr. Hielscher GmbH apparatus (ultrasonic horn S7, amplitude 88 μm , power density 300 W/cm^2 , frequency 24 kHz) for 2 hours and the temperature of ca 50°C.

The polyurethane (PU) non-woven membranes for MWNT dispersion filtration were prepared by technology of electrospinning from PU dimethyl formamide solution. For more details of PU chemical composition and particular process characteristics see reference [7]. To make entangled MWNT network on PU porous filtration membrane, the vacuum-filtration method was used. The formed network of disk shape was washed several times by deionized water (till neutral pH) and methanol in situ, then removed and dried between filter papers. The thickness of the disks was typically 0.15-0.4 mm (Fig. 1a).

The structure of MWNT network was investigated with a scanning electron microscope (SEM) made by Vega Easy Probe (Tescan s.r.o., Czech Republic). The sample was deposited onto the carbon targets and covered with a thin Au/Pd layer. The observation was carried out in the regime of secondary electrons.

Pure MWNT were also analyzed via transmission electron microscopy (TEM) using microscope JEOL JEM 2010 at the accelerating voltage of 160 kV. The sample for TEM was fabricated on 300 mesh copper grid with a carbon film (SPI, USA) from MWNT dispersion in acetone prepared by ultrasonication, which was deposited on the grid and dried.

The network tensile test was carried out using a simple set-up. The network stripe (length 45 and wide 10 mm) cut out from the manufactured disk of entangled carbon nanotube network was stepwise stretched increasingly with 20 sec delay of deformation reading in each step. The resistance/compression dependence for network stripes was measured during their compression between glass plates. The gap between the plates, which determines the network compressive deformation, was adjusted by calibrated metal spacer plates. The electric resistance along the stripe was measured by the two-point technique with multimeter Sefram 7338. The electrical contacts were fixed to the stripes by silver colloid electro-conductive paint Dotite D-550 (SPI Supplies).

3 Results and discussion

3.1 Experimental results

The MWNT aqueous dispersion was filtered through PU non-woven membrane to form intertwined network. As follows from Fig. 1, PU fibres of the membrane are straight with average diameter 0.14 ± 0.09 μm ranging between 0.05-0.39 μm . The fibre surface is smooth and the main pore size is around 0.2 μm . The typical thickness of prepared self-standing MWNT entangled networks (Fig. 2a) was about 0.15-0.65 mm. The upper surface of the network can be seen in SEM micrograph, Fig. 2b. Drying caused shrinkage of the network by about 7 %. The porosity of MWNT network was calculated to be $\langle f \rangle = 1 - p_{na} / p_{um:m}$,

where $p_{mi} = 0.56 \pm 0.03$ g/cm denotes the measured apparent density of the nano tube network ($n = 10$) and $PMWCUT^N-7$ g/cm³ is the measured average density of MWNT ($n = 3$). The nanotubes density is very close to the theoretical value for MWNT, i.e. 1.8 g/cm³ [8]. Also the network porosity very well corresponds to the published values for MWNT networks [9].

To determine dimension, parameters of used MWNT like their length, thickness and also to analyze their layer structure and possible structural defects TEM analysis was used. The proportions of MWWNT slightly differ from the properties declared by the manufacturer. The diameter of individual nanotubes was determined, to be between 10 and 60 nm, their length from tenths of micron up to 3 μ m. The maximum aspect ratio of the measured MWNT is thus about 300. A representative sample of nanotubes is shown in Fig. 3a. As usually, observation in multilayered tubes poses some structural defect. They can be adjusted as internal caps or closed compartments, or different kind of dislocation like edge dislocation-type, defect which can represent a changeover from scroll-like to "Russian doll" configuration [10,11]. The closer layer structure of used MWNT structure can be examined using high-resolution TEM mode. Fig. 3b. As can be seen, MWNT consists of concentric grapheme tubes (on image of about 15, typically from 10 to 35) with the interlayer distance of approx. 0.35 nm. The outer surface of MWNT is typically roughed. Such wrinkled surface can have origin in some carbon scotch material adhered onto tube surface, or as a projection of terminating graphene layers in scroll-like configuration of MWNT structure or as a defective outer walls created by tubes oxidation. As was proved in [12] using x-ray photoelectron spectroscopy, XPS, also pure material as delivered by producer, contains some oxygenated functional groups (mainly carboxylic functional but also significant amounts of other groups such as hydroxyl and carbonyl groups) which are product of oxidation. It happens immediately after production when tubes are exposed to environment.

Five network samples were tested for mechanical properties; the results of tensile test are shown in Fig. 4. The initial tensile modulus determined from the graph is about 650 MPa and the ultimate tensile strength 1 MPa.

The electric conductivity obtained by the four probe technique for different network thicknesses is presented in Fig. 5. As apparent from the graph, it increases with the network thickness from a very low value of 0.13 ± 0.01 S/cm at the thickness 17 μ m through 8.28 ± 0.01 S/cm at the thickness 23 μ m to almost constant values for the network thickness above 30 μ m. The measured conductivity for the network thickness 247 μ m was 22.9 ± 1.5 S/cm.

The pivotal property investigated in the research was resistance/compressive strain dependence. The measurements have shown that compression causes a decrease in MWNT network resistance, as clearly visible in Fig. 6. The plotted resistance values, R , are normalized with respect to the

initial resistance, R_0 , recorded at the start of the test. For each network thickness, i.e. 0.23 and 0.38 mm, four samples were investigated. Their resistance was measured after each compression step to the preset deformation and for the subsequent unloaded state. The resistance in the unloaded states was reduced similarly to the resistance of compressed samples. The graph indicates that the resistance change occurs in both the loaded and unloaded states. It can be seen that compression causes a permanent resistance change which becomes constant when the network is subjected to high compressive strain.

Further, the effect of repeated compression was followed. The plot of resistance vs. cyclic compression is presented in Fig. 7. As can be seen, with increasing number of deformation cycles the resistance of MWNT network first declines more steeply but after several cycles the decrease is very slight, and eventually no resistance change is observed. It indicates that during first deformations the nanotubes network get the structure which in both the loaded and the unloaded state is more or less the same regardless the number of deformation cycles.

3.2 Stochastic model of MWNT network resistance

The resistance of the MWNT network is affected by many factors ranging from nanotube conduction mechanisms through their size to contact resistance between nanotubes and the network architecture [13]. Networks investigated in our study are formed by randomly oriented short nanotubes. A similar research was carried out for short single wall carbon nanotubes (SWCNT) networks [14,15] with the result that the network resistance is dominated by the contact resistance between nanotubes while the intrinsic resistance of nanotubes is negligible. We adopt this picture also for MWNT network and moreover, we assume that the total resistance of the network is governed by the distribution of individual intercontact resistances. The study mentioned before [13] supposed a uniform distribution of the intercontact resistances for unloaded SWCNT network. In our case, it is assumed that the distribution of intercontact resistances in compressed MWNT network is such that the joint probability for this total network resistance change under strain s is described by the cumulative distribution function $F(s)$ for the two-parameter Weibull distribution

$$\Pr(\varepsilon) = F(\varepsilon) = 1 - \exp\left[-\left(\varepsilon/\varepsilon_0\right)^m\right]$$

where $F(s)$ is the cumulative distribution function of Weibull distribution. $F(s)$ is an increasing function, $0 < F(s) < 1$, and represents the probability of network resistance change $\Pr(\wedge)$ under strain no greater than s .

In accordance with the evidence given in [4], the local force between nano tubes increases during the compression. This allows better contacts between them, which consequently leads to the decrease of intercontact resistances. Besides electron transfer facilitated this way, the residual

resistance decrease shown in Fig. 6 suggests an additional mechanism of strain/resistance relation. As indicated in [15], compression may also bend the nanotubes sideways, which results in more contacts between nanotubes. Since the contact points act as parallel resistors, their increasing number causes reduction of overall network resistance. This structure reorganization, i.e. more contact points, probably partly remains when the compressive strength is released, which may be the reason for off-load resistance decrease.

The lack of detailed knowledge of the inner contact creation mechanism encourages us again to translate the results of experimental observation into the probabilistic scheme. Within the framework of this scheme, the on-load contact formation can be related to the site specific properties of an individual unit in the system of configurational units. The complementary cumulative distribution function (CCDF) for a stochastic scheme with a large system of configurational units undergoing transitions and with the distribution of macroscopic transition rate (in the strain domain) takes the only possible form of the one-sided Levy-stable distribution, that is, the stretched exponential [16-18]. The CCDF of Weibull distribution

$F_c(\varepsilon) = 1 - F(\varepsilon) = \exp\left[-(\varepsilon/\varepsilon_0)^n\right]$ chosen to represent the probability of the network resistance change under strain s due to intercontact resistance reduction is also a stretched exponential. Though the joint CCDF of two events in conjunction may not be a stretched exponential, the first- approximation model of the joint CCDF is chosen to be in this form. The measured inverse dependence of the macroscopic, i.e. whole network resistance on the compressive strain is in accordance with the chosen probability tendency. Consequently, the following relation of the probability function to the network resistance links appropriately the model deterministic prediction with the observed strain-dependent network resistance decrease,

$$R/R_0 = f(\varepsilon) = \exp\left[-(\varepsilon/a)^b\right]$$

The function $f(s)$ is expressed by the transition function equal to the stretched exponential CCDF $F(s)$. The reasonably good description of the measured data by the predictive relation (2), shown in Fig. 5 as a line (parameters $a=7.57$, $b=0.56$), justifies the probability model chosen here for the MWNT network resistance change under compression.

4 Final remarks

The strain/resistance relation for entangled carbon nanotube network structures of buckypaper produced by filtering a nanotube suspension has not been studied in details so far. Thus the primary

aim of this paper was to reveal the effect of compression on the network resistance when a simple and repeated loading is exerted. The measurements carried out have shown as much as 20% resistance reduction at the maximum applied deformation. When the compression load is released, the network resistance partially recovers. The recovery depends on the loading extent and history. For instance, the resistance recovery is constant when the preceding network compression was about 0.8 and nearly constant when the sample has been subjected to several compressive cycles (depending on compressive strain).

The overall network resistance change reflects the increase of local contact forces, i.e. better contact between nanotubes, which reduces the network resistance. Another considered mechanism contributing to the number of conducting contacts in the course of compression is bending of nanotubes sideways. Since the contact points act as parallel resistors, their higher number results in reduced total network resistance. Both mechanisms are deterministic physical processes caused by loading applied crosswise the network sheet. These processes involve both decrease of the resistance of existing contacts and creation of new ones during compression. However, due to the lack of knowledge of these deterministic processes, in this study we apply the probability description of events. It leads to the first-approximation model of joint inner mechanisms of compressive strain effect on the overall resistance of nanotubes network. The choice of the probability model is justified by reasonably good agreement between the resistance/strain dependence given by equation (2) and shown in Fig. 6, and the experimental results for the electrical properties dependence on mechanical deformation of carbon nanotube network.

Acknowledgement This project was financially supported by the Ministry of Education, Youth and Sports of the Czech Republic (MSM 7088352101), the Grant Agency of the Academy of Sciences of the Czech Republic (GA AV IAA200600803) and by the Fund of Institute of Hydrodynamics AV0Z20600510.

References

1. E.T. Thostenson, C.Y. Li, T.W. Chou: *Compos. Sci. Technol.* **65**, 491 (2005)
2. Q. Cao, J.A. Rogers: *Adv. Mater.* **21**, 29 (2009)
3. D.A. Walters, M.J. Casavant, X.C. Quin, C.B. Huffman, R.J. Boul, L.M. Ericson, E.H. Haroz, M.J. O'Connell, K. Smith, D.T. Colbert, R.E. Smalley: *Chem. Phys. Lett.* 338, 14 (2001)
4. A. Allaoui, S.V. Hoa, P. Evesque, J. Bai: *Scripta Mater.* **61**, 628 (2009)
5. H.T. Ham, Y.S. Choi, I.J. Chung: *Colloid Interf. Sci.* **286**, 216 (2005)
6. C.S. Chern, L.J. Wu: *Polym. Sci., Part A: Polym. Chem.* **39**, 3199 (2001)

7. D. Kimmer, P. Slobodian, D. Petras, M. Zatloukal, R. Olejnik, P. Saha: *J. Appl. Polym. Sci.* **III**, 2711(2009)
8. X.L. Xie, Y.W. Mai, X.P. Zhou : *Mater. Sci. Eng. R* **49**, 89 (2005)
9. R.L.D. Whitby, T. Fukuda, T. Maekawa, S.L. James, S.V. Mikhalovsky: *Carbon* **46**, 949 (2008)
10. Harris P.J.F., *Carbon Nanotube Science, Synthesis, properties and applications*, Cambridge University Press, New York 2009
11. J.G. Lavin, S. Subramoney, R.S. Ruoff, S. Berber, D. Tomanek, *CARBON* **40**, 1123 (2002)
12. L. Licea-Jimenez, P.Y. Henrio, A. Lund, T.M. Laurie, S.A. Perez-Garcia, L. Nyborg, H. Hassander, H. Bertilsson, R.W. Rychwalski, *Composites Science and Technology* **67**, 844, (2007)
13. C.S. Yeh: *A Study of Nanostructure and Properties of Mixed Nanotube Buckypaper Materials: Fabrication, Process Modeling Characterization, and Property Modeling*, Ph.D. Thesis, The Florida State University (2007)
14. D. Hecht, L. Hu, G. Gruener: *Appl. Phys. Lett.* **89**, 133112 (2006)
15. O. Yaglioglu, A.J. Hart, R. Martens, A.H. Slocum: *Rev. Sci. Instrum.* **77**, 095105 (2006)
16. A.K. Jonscher, A. Jurlewicz, K. Weron: *Contemp. Phys.* **44**, 329 (2003)
17. A. Jurlewicz, K. Weron: *Cell Mol. Biol. Lett.* **4**, 55 (1999)
18. A. Jurlewicz, K. Weron: *J. Non-Cryst. Solids* **305**, 112 (2002)

FIGURE CAPTURES

Fig.1 SEM micrographs of PU non-woven filtering membrane

Fig. 2 a) Free-standing randomly entangled MWNT network (disk diameter 75 mm, thickness 0.15 mm), b) SEM image of the surface of entangled MWNT network of buckypaper.

Fig. 3 a) TEM image of MWNT deposited on the filter, b) HRTEM detailed view of the structure of the nanotube.

Fig. 4 Stress/strain dependence for MWNT network in tensile test (network thickness 0.38 mm). Data presented as a mean \pm standard deviation, $n = 5$.

Fig. 5 The effect of thickness of the entangled carbon nanotube network structures of buckypaper on the electric conductivity.

Fig. 6 Normalized resistance vs. strain dependence of entangled carbon nanotube network. The

network thickness is 0.23 mm (squares) and 0.38 mm (circles). The full and open symbols denote the network with and without load, respectively. Data presented as a mean \pm standard deviation, $n = 4$. The solid line represents the prediction given in equation (2).

Fig. 7 The normalized resistance of the entangled carbon nanotube network vs. the number of compression-relaxation cycles; network thickness 0.38 mm. The applied compressive strain: 0.21 (circles), 0.47 (squares) and 0.74 (triangles). Full and open symbols denote the network with and without load, respectively.

Fig. 1

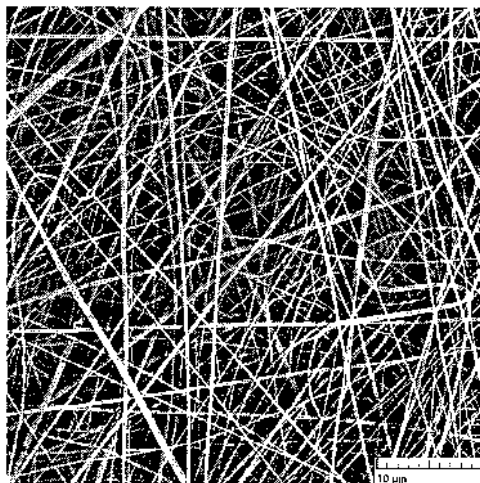


Fig. 2

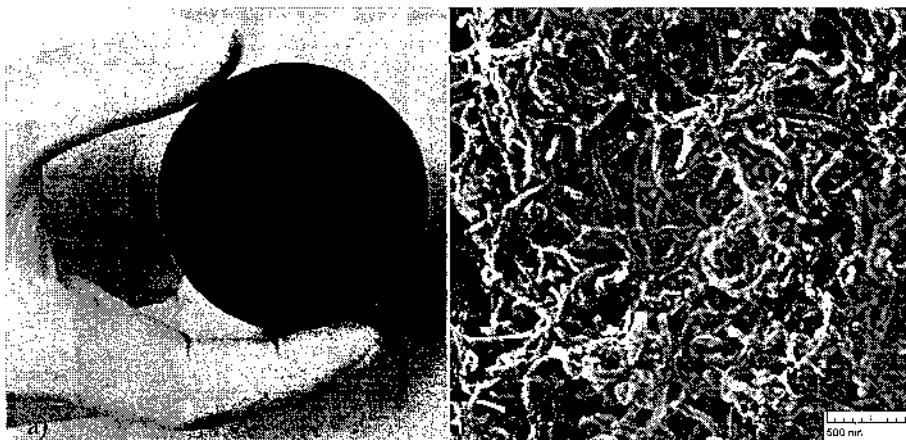


Fig. 3

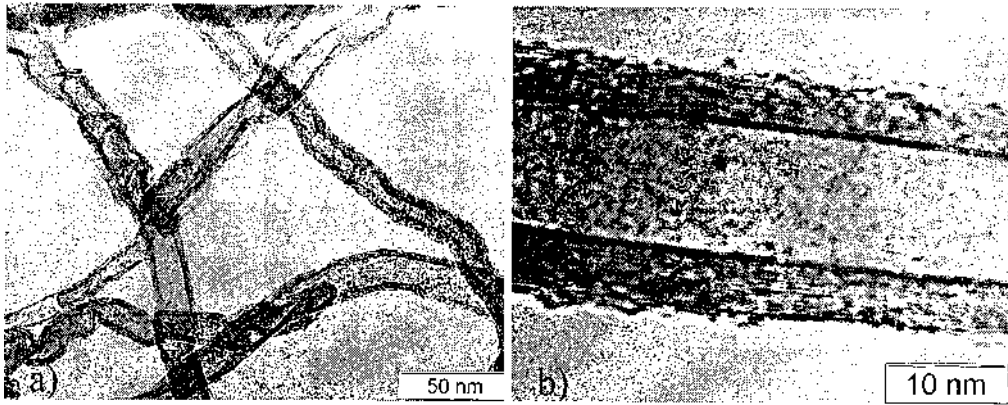


Fig. 4

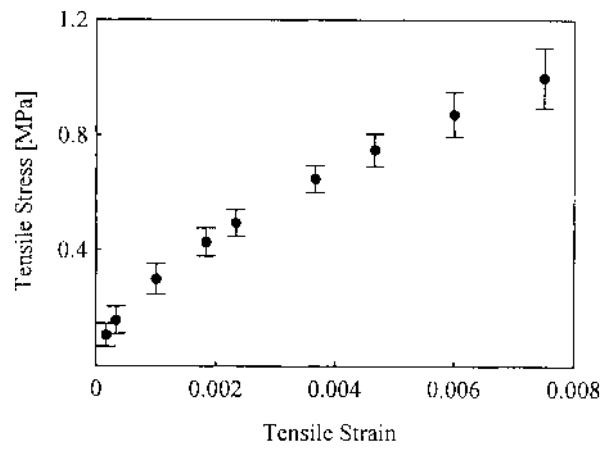


Fig. 5

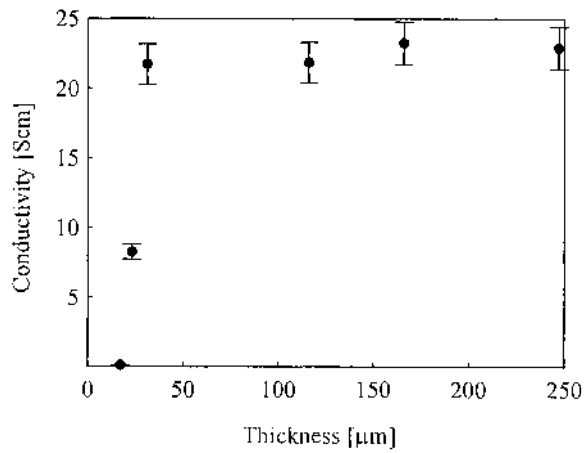


Fig. 6

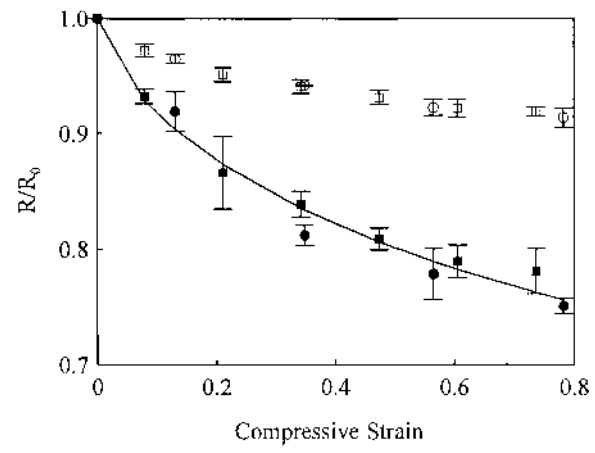


Fig. 7

